Available online at www.sciencedirect.com
ScienceDirect
Mendeleev Commun., 2014, **24**, 316–318

Mendeleev
Communications

Effect of introduced zeolite on the Fischer–Tropsch synthesis over a cobalt catalyst

Lilia V. Sineva,*[a,b] Ekaterina Yu. Khatkova,[a,c] Ekaterina V. Kriventseva[a] and Vladimir Z. Mordkovich[a,b]

[a] *Technological Institute for Superhard and Novel Carbon Materials, 142190 Troitsk, Moscow, Russian Federation. Fax: +7 499 400 6260; e-mail: sinevalv@tisnum.ru*
[b] *INFRA Technology Ltd., 125009 Moscow, Russian Federation*
[c] *Department of Chemistry, M. V. Lomonosov Moscow State University, 119991 Moscow, Russian Federation*

DOI: 10.1016/j.mencom.2014.09.024

A mean distance between zeolite and cobalt particles in Fischer–Tropsch catalysts is an important factor affecting the activity of a multicomponent catalyst bed.

The Fischer–Tropsch synthesis (FTS) is as an alternative technology for producing high-quality synthetic oil from carbon-containing feedstock such as natural gas, associated gas, shale gas, coal or biomass, and its development is very important.[1,2]

Cobalt FTS catalysts produce sulfur-free synthetic oil with a wide fraction of predominantly linear hydrocarbons, where branched and unsaturated hydrocarbons (mostly α-olefins) may occur.[2,3] The advantage of using skeleton cobalt in FTS over conventional impregnated cobalt systems is its high thermal conductivity.[4] This is important because the process is highly exothermic and heat removal from the reaction zone is necessary.

The FTS products formed at the metal sites of the catalyst may participate in secondary reactions at the acid sites of zeolites or mixed oxides.[5–7] For example, olefins or their intermediates can migrate to acid sites and undergo isomerization and/or hydroisomerization, while alkanes can undergo cracking or hydrocracking. It is likely that the composition of produced hydrocarbon mixtures depends on the ratio of reaction rates at acid and metal sites.

For better understanding the relative contributions of primary and secondary reactions to the formation of hydrocarbons, it is reasonable to study fixed catalyst beds with different arrangements of cobalt and zeolite particles.

The aim of this work was to determine the role of zeolite in the production of synthetic oil (a mixture of liquid hydrocarbons with a boiling point below 450 °C) from CO and H_2 in the presence of skeleton cobalt. The highly dispersed skeleton cobalt was prepared from a CoAl alloy.[8] Table 1 summarizes the experimental setups of catalyst beds used in the experiments.[†] Table 2 represents the optimal synthesis temperatures for all of the test catalytic beds at different GHSVs.

Table 1 Test catalyst fixed beds.

Bed setup	Composition (wt%)			
	Co	Al	HBeta	AlO(OH)
Co[a]	22	55	0	23
Co–Z[b]	20	50	10	20
Co+Z[c]	20	50	10	20
$(Co+Z)_{pel}$[d]	20	50	10	20

[a] A layer of the cobalt-containing mixture 4 cm in height with a thermocouple located in the upper third of the layer. [b] A layer of the cobalt-containing mixture, a layer of quartz sand 5 mm in height and a layer of zeolite 6 cm in height with two thermocouples located 0.5 cm from the top and the bottom of the bed, respectively. [c] A layer of zeolite uniformly mixed with the cobalt-containing mixture (the mean distance between cobalt and zeolite particles was tens of micrometers) 4 cm in height with a thermocouple located in the upper third of the layer. [d] The composition is the same as that in Co+Z. A layer of pelletized zeolite and the cobalt-containing mixture[9] (the mean distance between cobalt and zeolite particles was several micrometers) 3 cm in height with a thermocouple located in the upper third of the layer.

Table 2 Optimum synthesis temperatures.

GHSV/h^{-1}	Temperature/°C			
	Co	Co–Z	Co+Z	$(Co+Z)_{pel}$
3000	251	258	258	234
5000	264	269	264	240

All of the catalytic beds demonstrated activity in the FTS (Figure 1). The introduction of a separate zeolite layer (Co–Z bed) leads to a decrease in the conversion of CO (compared with the Co bed), which is more significant at 3000 h^{-1} GHSV (from 54 to 33%). This may be due to the fact that highly dispersed zeolite particles are located between larger quartz particles to result in a layer compaction which prevents the removal of heavy viscous hydrocarbons from the cobalt-containing layer located

---

[†] All the setups were based on cobalt-containing mixtures containing the skeleton cobalt, highly dispersed aluminum metal powder and boehmite, which was precalcined in air at 450 °C. Zeolite HBeta (Z) was used in three setups as an additive or as a separate layer (see Table 1). The mixtures were uniformly mixed with quartz sand in a weight ratio 1 : 4 before loading into the reactor bed. The particle sizes were <45 μm for aluminum powder, 4–5 μm for boehmite, 1–2 μm for zeolite HB, about 2.8×0.9–12×7 μm for Raney cobalt and 0.1–0.3 mm for quartz sand.

The catalyst was activated in pure hydrogen, which was supplied at a gas-hour space velocity (GHSV) of 3000 h^{-1} at 400 °C and 0.1 MPa for 1 h. The synthesis was carried out in a steel flow reactor (25 cm in length with an inner diameter of 1 cm) equipped with four thermocouples at distances of 5 cm. After activation, the catalyst was heated from 170 to 231–235 °C in 3–10 °C steps at regular intervals of 6 h in a synthesis gas flow (gas pressure, 2 MPa). Synthesis gas (H_2/CO molar ratio of 2 with 5 vol% N_2 as the balance and internal reference) was supplied at a GHSV of 1000 h^{-1}. The temperature was varied to reach a maximum liquid yield; then, GHSV was increased stepwise up to 5000 h^{-1} to optimize the yield of C_{5+} hydrocarbons.

The composition of the products was determined by gas chromatography. A column with molecular sieves CaA (3 m × 3 mm) was used for the separation of CO and CH_4; a HayeSep column (3 m × 3 mm) was used for the separation of CO_2 and C_2–C_4 hydrocarbons, and a 50 m capillary column with DP-Petro plate was used for the separation of C_5–C_{29} hydrocarbons.

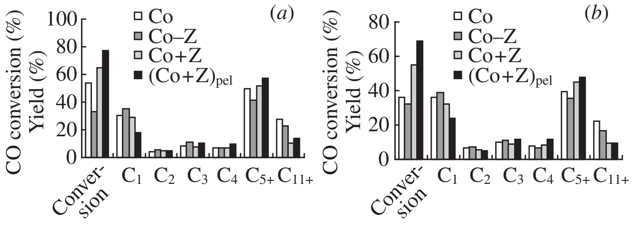

Figure 1 The effect of catalyst composition on CO conversion and yield of hydrocarbons at (*a*) 3000 and (*b*) 5000 h^{-1} at optimal synthesis temperatures (Table 2).

above; thus, it obstructs the supply of feed components (CO and H_2) to active metal sites. An increase in the synthesis gas flow rate up to 5000 h^{-1} decreased the conversion of CO to 37% even in the case of a Co bed (no zeolite barrier effect).

A uniform zeolite distribution in the layer of cobalt-containing powder (Co+Z bed) significantly increased the conversion of CO to 65% at 3000 h^{-1} or to 56% at 5000 h^{-1}, while pelletizing [$(\mathrm{Co+Z})_{\mathrm{pel}}$ bed] led to its increase up to 77% at 3000 h^{-1} or 69% at 5000 h^{-1} (Figure 1). Moreover, in the presence of $(\mathrm{Co+Z})_{\mathrm{pel}}$, the yield of C_{11+} hydrocarbons decreased from 22–28 to 10–14% at 3000 h^{-1} or from 17–22 to 10% at 5000 h^{-1}. Thus, it is believed that a shorter cobalt–zeolite interparticle distance [a drop from tens of μm in Co+Z down to several μm in $(\mathrm{Co+Z})_{\mathrm{pel}}$] promotes the easier and faster removal of heavy hydrocarbons from active metal sites and vacates these sites for the adsorption of feed components. Furthermore, a shorter cobalt–zeolite interparticle distance leads to the more active formation of hydrocarbons due to a decrease in the average molecular weight of the produced hydrocarbons. Note that the yield of C_{5+} hydrocarbons significantly decreased at either of the synthesis gas flow rates (Figure 1).

The yield of methane slightly increased from 31–37% in the presence of the Co bed to 35–39% with the introduction of a separate zeolite layer (Co–Z); this can be due to cracking reactions proceeding at zeolite sites. The reduction of the cobalt–zeolite interparticle distance results in a decrease in the yield of methane to 18–23% in the presence of the pelletized sample. It can be assumed that the mechanism of secondary reactions on zeolite depends on the distance between zeolite and cobalt active sites.[10–16] The yield of C_2 hydrocarbons is a function of the cobalt–zeolite interparticle distance (Figure 1).

The yield of C_3 hydrocarbons increased upon the introduction of a separate zeolite layer in (Co–Z) as well as in the presence of the pelletized $(\mathrm{Co+Z})_{\mathrm{pel}}$ and decreased in the mixed-powder Co+Z bed (Figure 1). Therefore, it is likely that the formation of C_3 hydrocarbons depends on mass transport limitations.

Figure 2 represents the dependence of the composition of C_4 hydrocarbons on catalyst bed composition. At 3000 h^{-1}, *n*-butane (0.54) and *n*-butylene (0.41) were the main C_4 compounds produced over the Co bed setup, while the isobutane content was only 0.05, and isobutylene was not formed. Therefore, we observed a traditional SFT pattern.[17,18] A separate zeolite layer in Co–Z led to a slight increase in the *n*-butane content (to 0.58), a significant decrease in the *n*-butylene (to 0.19) and increase in the isobutane (to 0.19) contents and the appearance of isobutylene (0.04). The *n*-butylene formed on cobalt sites undergoes readsorption on the zeolite layer and isomerization as suggested previously.[19] The mixing of cobalt and zeolite in Co+Z resulted in an increase in the *n*-butane content (to 0.7), a further decrease in the amount of *n*-butylene and a significant decrease in the amount of iso products [Figure 2(*a*)]. The most probable explanation suggests that the hydrocarbons produced at the metal sites undergo cracking into olefins over zeolite.[3,20] Then, the olefins undergo readsorption on metal sites followed by hydrogenation and hydrocracking or the initiation of hydrocarbon chain growth.[21] Pelletized $(\mathrm{Co+Z})_{\mathrm{pel}}$ led to a decrease in the *n*-butane content (to 0.64) and an insignificant increase in the *n*-butylene, isobutylene and isobutane contents (to 0.19, 0.04 and 0.13, respectively). This can be due to diffusion limitations, which influence mass transfer in a pellet and prevent cracked products from readsorption on cobalt-containing sites.

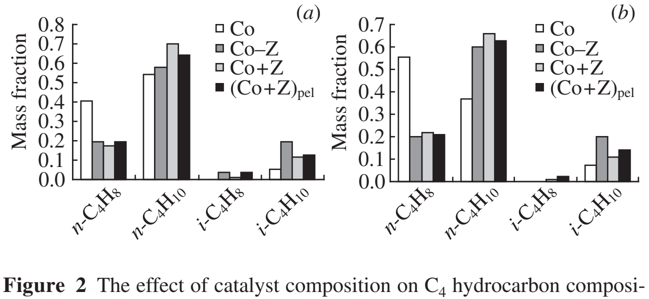

Figure 2 The effect of catalyst composition on C_4 hydrocarbon composition at (*a*) 3000 and (*b*) 5000 h^{-1} at optimal synthesis temperatures (Table 2).

The distribution of C_4 products slightly changed as contact time was shortened due to an increase in the synthesis gas flow rate [Figure 2(*b*)]. Thus, in the presence of the Co bed setup, the *n*-butane content decreased (to 0.38), while the *n*-butylene content increased (to 0.56). The isobutane content raised insignificantly, while isobutylene was not formed. It is obvious that a shorter contact time prevents the hydrogenation of *n*-olefins, which are routinely produced from CO and H_2 as the FTS products. The introduction of a separate zeolite layer in Co–Z had almost no effect on the distribution of C_4 hydrocarbons with the exception of isobutylene, which did not appear in the product. An increase in the synthesis gas flow rate for this zeolite and cobalt configuration seems to prevent *n*-butylene from participating in secondary reactions.

As for the group composition of the liquid products formed at 3000 h^{-1}, the Co bed afforded hydrocarbons containing 82% linear alkanes, 11% olefins and 7% isoparaffins. The introduction of a zeolite layer into Co–Z led to a decrease in the *n*-paraffin content (to 74%) and an increase in the olefin content (to 18%), while the concentration of isoparaffins remained almost unchanged (8%). This product composition can result from the cracking of C_{5+} hydrocarbons (produced on cobalt active sites) on zeolite active sites. It is well known[22] that cracking can occur on H-form zeolite under FTS conditions.

The uniform distribution of zeolite and cobalt particles in Co+Z results in a drastic decrease in the *n*-paraffin content (to 47%) and an increase in both olefin and isoparaffin contents (to 25 and 18%, respectively). In other words, a contribution of cracking and isomerization processes seems plausible under such conditions,[23] and the probability of such reactions to occur grows with reducing distance between cobalt and zeolite sites as a result of a prolongation of the contact time of a high-molecular-weight film formed on cobalt and zeolite sites. Pelletized $(\mathrm{Co+Z})_{\mathrm{pel}}$ promoted the formation of isoparaffins (23%) at the expense of the *n*-paraffin content (42%). Thus, diffusion limitations at 3000 h^{-1} seem to promote isomerization reactions.

At 5000 h^{-1}, the introduction of a separate zeolite layer in Co–Z caused a similar shift (compared to 3000 h^{-1}) in the group composition of produced hydrocarbons: the olefin and isoparaffin contents increased from 15 to 26 and from 8 to 11%, respectively, while the *n*-paraffin content decreased from 77 to 63%. The hydrocarbons produced over Co+Z at the above flow rate were characterized by the same group composition as that on Co–Z: 24% olefins, 16% isoparaffins and 60% *n*-paraffins. This effect correlates with the fact that a higher flow rate reduces the probability of the readsorption of cracking products in the case of Co+Z. In the pelletized bed $(\mathrm{Co+Z})_{\mathrm{pel}}$, the C_{5+} hydrocarbons contained 39% olefins, 19% isoparaffins and 42% *n*-paraffins regardless of flow rates.

A comparison of the molecular-weight distributions of C_8–C_{27} hydrocarbons helps us to understand the fractional composition of liquid products (Figures S1 and S2, Online Supplementary Materials). In particular, the Co and Co–Z bed setups provide very similar distributions at 3000 h^{-1}. The uniform mixture of cobalt and zeolite powders Co + Z gave a significant shift in the C_8–C_{27} molecular-weight distribution; *i.e*., the concentration of hydrocarbons with boiling points below 170 °C raised; the diesel fraction content decreased, and hydrocarbons with more than 25 carbon atoms in molecules were formed in trace amounts. It is obvious that, in this case, the distance between cobalt and zeolite particles does not affect the contact time of a high-molecular-weight film formed on cobalt sites with zeolite sites. The influence of diffusion limitations results in diminishing the low-boiling hydrocarbon content and rising the high-boiling fraction content [Figure S2(*a*)]. However, note that, despite the increase in the heavy hydrocarbon content, the heaviest detected hydrocarbon contained only 23 carbon atoms.

The Co–Z bed setup was most sensitive to flow rate [Figure S2(*b*)]. The C_8–C_{11} hydrocarbon content increased significantly, while the C_{12}–C_{27} hydrocarbon content decreased. Probably, the higher synthesis gas flow rate and synthesis temperature (Table 2) resulted in the higher rates of secondary reactions. It is interesting that the extraction of the Co bed from the reactor showed a large quantity (> 3 g) of white creamy hydrocarbons with a typical wax odor. Such products were not detected in the presence of zeolite-containing bed setups; however, the porous structure of the pellets accumulated small amounts of hydrocarbons and intermediates, which are difficult to identify. Products obtained in the presence of the pelletized catalyst were analyzed by the SimDist method in the Saybolt laboratory; the end of boiling at 416 °C was detected, which corresponds to $C_{26}H_{58}$ (see Online Supplementary Materials).

Thus, we found that the influence of zeolite on the synthesis of hydrocarbons from CO and H_2 in the presence of skeleton cobalt is governed by not only the acidic properties of the zeolite but also the mean cobalt–zeolite interparticle distance. Sartipi *et al*.[10] studied a combination of HZSM-5 zeolite and an active cobalt phase in FTS (260 °C, 10 atm and $H_2/CO = 1.25$–2.25) and found that the activity of the bifunctional catalytic system correlates with the proximity of cobalt and zeolite phases. We observed that the closer were placed zeolite and cobalt particles to each other, the more active was the catalyst. It is obvious that secondary transformations of high-molecular-weight products accelerate with reducing distance between zeolite and cobalt particles. This results in a decrease in the average molecular weight of products, which facilitates mass transfer both in a mixture of powders and in a pellet.[5]

At the same time, we observed an increase in the concentration of branched and unsaturated hydrocarbons and a decrease in the *n*-paraffin content down to 40%. It is believed that the hydrocarbons formed on metal sites undergo cracking on the acid sites of zeolite. According to published data,[3,20] cracking occurs by a carbocation mechanism with the formation of shorter hydrocarbon chains, olefins and isoparaffins. Moreover, heavier hydrocarbons are involved in cracking transformations. For this reason, we did not observe the formation of heavy hydrocarbons even in the case of a layered bed setup.

Therefore, the role of zeolite in hydrocarbons formation from CO and H_2 in the presence of skeleton cobalt has been revealed and the zeolite effect on the products composition has been shown. The mean distance between zeolite and cobalt particles is an important factor affecting the activity of multicomponent catalyst bed.

Online Supplementary Materials

Supplementary data associated with this article can be found in the online version at doi:10.1016/j.mencom.2014.09.024.

References

1 V. S. Arutyunov and R. N. Magomedov, *Russ. Chem. Rev*., 2012, **81**, 790.

2 *Greener Fischer–Tropsch Processes*, eds. P. M. Maitlis and A. Klerk, Wiley–VCH, Weinheim, 2013, p. 372.

3 A. P. Steynberg and M. E. Dry, *Fischer–Tropsch Technology*, Elsevier, 2004, vol. 64, p. 722.

4 L. V. Sineva, V. Z. Mordkovich and E. Yu. Khatkova, *Mendeleev Commun*., 2013, **23**, 44.

5 J. Cejka, A. Corma and S. Zones, *Zeolites and Catalysis*, Wiley-VCH, Weinheim, 2010, p. 881.

6 B. Sun, M. Qiao, K. Fan, J. Ulrich and F. Tao, *ChemCatChem*, 2011, **3**, 542.

7 A. L. Lapidus, M. V. Tsapkina, A. Yu. Krylova and B. P. Tonkonogov, *Russ. Chem. Rev*., 2005, **74**, 577 (*Usp. Khim*., 2005, **74**, 634).

8 A. V. Khykhrik, *PhD Thesis*, 2001 (in Russian).

9 V. Z. Mordkovich, L. V. Sineva, I. G. Solomonik, V. S. Ermolaev and E. B. Mitberg, *Patent WO 2010/147513 (A2)*, 2010.

10 S. Sartipi, J. E. van Dijk, J. Gascon and F. Kapteijn, *Appl. Catal., A*, 2013, **456**, 11.

11 J. He, Z. Liu, Y. Yoneyama, N. Nishiyama and N. Tsubaki, *Chem. Eur. J*., 2006, **12**, 8296.

12 X. Li, J. He, M. Meng, Y. Yoneyama and N. Tsubaki, *J. Catal*., 2009, **265**, 26.

13 X. Huang, B. Hou, J. Wang, D. Li, L. Jia, J. Chen and Y. Sun, *Appl. Catal., A*, 2011, **408**, 38.

14 C. Li, H. Xu, Y. Kido, Y. Yoneyama, Y. Suehiro and N. Tsubaki, *ChemSusChem*, 2012, **5**, 862.

15 B. Sun, G. Yu, J. Lin, K. Xu, Y. Pei, S. Yan, M. Qiao, K. Fan, X. Zhang and B. Zong, *Catal. Sci. Technol*., 2012, **2**, 1625.

16 R. Oukaci, J. C. S. Wu and J. G. Goodwin, *J. Catal*., 1988, **110**, 47.

17 A. B. Fontenelle, Jr. and F. A. N. Fernandes, *Chem. Eng. Technol*., 2011, **34**, 963.

18 G. P. Laan, *PhD Thesis*, ch. 2, 1999.

19 (*a*) U. A. Sedran, *Catal. Rev.-Sci. Eng*., 1994, **36**, 405; (*b*) Y. Jin, R. Yang, Y. Mori, J. Suna, A. Taguchic, Y. Yoneyama, T. Abec and N. Tsubakia, *Appl. Catal., A*, 2013, **456**, 75; (*c*) S. K. Saxena, N. Viswanadham and M. O. Garg, *Fuel*, 2013, **107**, 432.

20 (*a*) K. Cheng, J. Kang, S. Huang, Z. You, Q. Zhang, J. Ding, W. Hua, Y. Lou, W. Deng and Y. Wang, *ACS Catal*., 2012, **2**, 441; (*b*) M. L. Poutsma, in *Zeolite Chemistry and Catalysis*, ed. A. Rabo, Am. Chem. Soc. Monography, Washington, 1976, vol. 171, p. 437; (*c*) A. L. Lapidus and A. Yu. Krylova, *Russ. Chem. Rev*., 1998, **67**, 941 (*Usp. Khim*., 1998, **67**, 1032).

21 (*a*) A. L. Lapidus, A. Yu. Krylova, Ya. V. Mikhailova, L. V. Sineva and A. B. Erofeev, *Solid Fuel Chem*., 2011, **45**, 71 (*Khim. Tverd. Topl*., 2011, no. 2, 3); (*b*) A. A. Adesina, R. R. Hudgins and P. L. Silveston, *J. Appl. Catal*., 1990, **62**, 295; (*c*) A. L. Lapidus, A. Yu. Krylova, L. V. Sineva and Ya. V. Dyrandina, *Solid Fuel Chem*., 1998, **32**, 39 (*Khim. Tverd. Topl*., 1998, no. 2, 39).

22 (*a*) A. Martínez, J. Rollán, M. A. Arribas, H. S. Cerqueira, A. F. Costa and E. F. S. Aguiar, *J. Catal*., 2007, **249**, 162; (*b*) A. Freitez, K. Pabst, B. Kraushaar-Czarnetzki and G. Schaub, *Ind. Eng. Chem. Rev*., 2011, **50**, 13732; (*c*) A. M. Subiranas and G. Schaub, *Int. J. Chem. React. Eng*., 2009, **7**, A31; (*d*) J. Kang, K. Cheng, L. Zhang, Q. Zhang, J. Ding, W. Hua, Y. Lou, Q. Zhai and Y. Wang, *Angew. Chem. Int. Ed*., 2011, **50**, 5200.

23 (*a*) V. U. S. Rao and R. J. Gormley, *Catal. Today*, 1990, **6**, 207; (*b*) A. van Rustraat, *Adsorption Effect in Acid Catalysis by Zeolites*, Eindhoven University of Technology, 1997, p. 126; (*c*) J. I. Villegas, N. Kumar, T. Heikkilä, V.-P. Lehto, T. Salmi and D. Yu. Murzin, *Chem. Eng. J*., 2006, **120**, 83; (*d*) X. Li, K. Asami, M. Luo, K. Michiki, N. Tsubaki and K. Fujimoto, *Catal. Today*, 2003, **84**, 59.

Received: 10th December 2013; Com. 13/4267